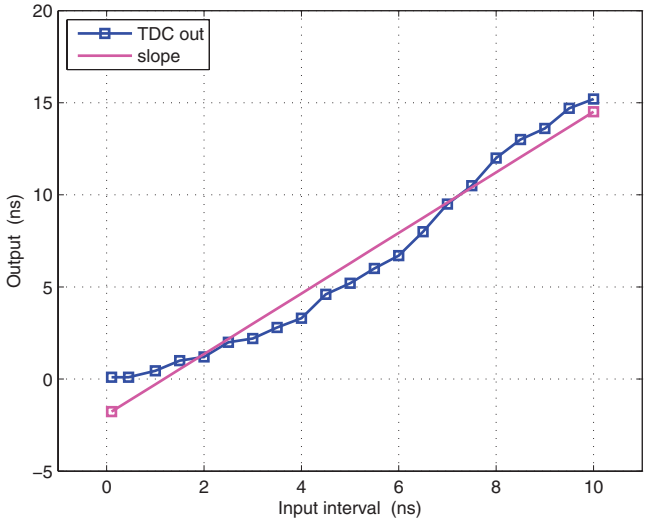

Figure 4 TDC output versus time interval of FOG. [Color figure can be viewed in the online issue, which is available at www.interscience.wiley.com]

To verify our idea of time interpolation within one clock period using dedicated carry lines, a simplified TDC based on counter and time interpolation methods was implemented in an FPGA. The block diagram of the simplified TDC is shown in Figure 3. Dedicated carry lines of an FPGA are used as delay cells to perform time interpolation within the system clock period and to realize the fine time measurement. Two gray-code counters, working on in-phase and out-of-phase system clocks, respectively, are designed to get the stable value of the coarse time measurement. The fine time code and the coarse time counter value, along with the channel identifier, are then written into a first-in first-out (FIFO) buffer. Experiments have been done to verify the performance of the TDC. Figure 4 shows the output response of TDC. Thus, we will obtain angular velocity from Eq. (9).

4. CONCLUSION

We have successfully constructed a coupled resonator fiber-optic gyroscope system using the slow light and time interval measurement for the first time. The investigations demonstrate the feasibility of achieving high sensitive fiber optic gyroscope for navigation purposes. This novel gyroscope will have all-solid configuration, compact size, and is also expected to achieve high resolution than conventional fiber-optic gyroscope. This method is a new direction for designing high-performance FOG in practical applications.

ACKNOWLEDGMENTS

The work of Y. Li was supported by the scientific research starting foundation for Returned Overseas Chinese Scholars, Ministry of Education.

REFERENCES

1. M.S. Bigelow, N.N. Lepeshkin, and R.W. Boyd, Observation of ultraslow light propagation in a ruby crystal at room temperature, Phys Rev Lett 90 (2003).
2. P. Chao, Z. Li, and A. Xu, Rotation sensing based on a slow-light resonating structure with high group dispersion, Appl Opt 46 (2007), 4125–4131.
3. U. Leonhardt and P. Piwnicki, Ultrahigh sensitivity of slow-light gyroscope, Phys Rev A 62 (2000).
4. M.S. Shahriar, G.S. Pati, R. Tripathi, V. Gopal, M. Messall, and K. Salit, Ultrahigh enhancement in absolute and relative rotation sensing using fast and slow light, Phys Rev A 75 (2007).
5. B.Z. Steinberg, Rotation photonic crystals: A medium for compact optical gyroscopes, Phys Rev E 71 (2005).
6. A.B. Matsko, A.A. Savchenkov, V.S. Ilchenko, L. Maleki, Optica gyroscope with whispering gallery mode optical cavities, Opt Commun 233 (2004), 107–112.
7. J. Scheuer and A. Yariv, Sagnac effect in coupled-resonator slow-light waveguide structures, Phys Rev Lett 96 (2006).
8. J. Song, Q. An, and S.B. Liu, A high-resolution time-to-digital converter implemented in field-programmable-gate-arrays, IEEE Trans Nucl Sci 53 (2006), 236–241.
9. C.K. Madsen and G. Lenz, Optical all-pass filters for phase response design with applications for dispersion compensation, IEEE Photon Technol Lett 10 (1998), 994–996.
10. E.J. Post, Sagnac effect, Rev Mod Phys 39 (1967), 475–493.
11. P. Chen, C.C. Chen, J.C. Zheng, and Y.S. Shen, A PVT insensitive vernier-based time-to-digital converter with extended input range and high accuracy, IEEE Trans Nucl Sci 54 (2007), 294–302.
12. J. Kalisz, Review of methods for time interval measurements with picosecond resolution, Metrologis 41 (2004), 17–32.

FABRICATION OF A NEW-TYPE WIDEBAND BANDPASS FILTER ON THE $MGTA_{1.5}NB_{0.5}O_6$ CERAMIC SUBSTRATE

Chien-Min Cheng,[1] Ying-Chung Chen,[1] and Cheng-Fu Yang[2]
[1] Department of Electrical Engineering, National Sun Yat-Sen University, Kaohsiung, Taiwan, Republic of China; Corresponding author: ccmin@mail.stut.edu.tw
[2] Department of Chemical and Materials Engineering, National University of Kaohsiung, Kaohsiung, Taiwan, Republic of China

Received 5 April 2008

ABSTRACT: *To enhance performance of microwave filter, one of the most effective methods is to insert transmission zeros in the stop-bands. A modified end-coupled microstrip line structure is combined with a hairpin resonator in this research. Using the combination technique and cross coupling, a miniature wideband microstrip bandpass filter is proposed on the $MgTa_{1.5}Nb_{0.5}O_6$ microwave dielectric ceramic substrate.* © 2008 Wiley Periodicals, Inc. Microwave Opt Technol Lett 50: 3223–3225, 2008; Published online in Wiley InterScience (www.interscience.wiley.com). DOI 10.1002/mop.23943

Key words: *$MgTa_{1.5}Nb_{0.5}O_6$ ceramic; wideband bandpass filter; end-coupled; hairpin*

1. INTRODUCTION

Microstrip line filters have found wide applications in RF and microwave circuits and many modified methods were used to improve the characteristics of microstrip line filters. In [1], the authors used inline stepped-impedance resonators (SIR) and cross coupling technique to accomplish a single-band filter and the first harmonic could be pushed to $4f_0$. In [2], the authors fabricated a wide-band filter on the RO3003 substrate with an operating frequency of 5 GHz and a bandwidth of 20%, and the response of pass band was affected by the variation of impedance. And in [3], the authors used λ/2 SIR resonators to accomplish dual-band (2.45/5.2 GHz) filters by the parallel-coupled microstrip line structures, and the bandwidth of the filters was controllable by the variation of coupling. In [4], the authors modified the parallel-coupled bandpass filters, and the transmission zeros beside the

operating frequency could be controlled independently. All of the above filters were fabricated on the RO substrates; however, there were few reports about the microwave devices developed on the microwave ceramic substrates. In this article, the end-coupled microstrip line structure was combined with a high impedance λ/2 cross coupling resonator [5], a new type of miniature microstrip dual-band filter was developed on the $MgTa_{1.5}Nb_{0.5}O_6$ (MTN) microwave dielectric ceramic substrates [6]. The MTN ceramic exhibited high dielectric constant ($\varepsilon_r = 27.9$) that would decrease the size of filters and high quality factor ($Q \times f = 33{,}100$ GHz) that would improve the characteristics of the filters obviously. The design procedures and the characteristics of the filters would be well investigated.

2. THE DESIGNED PROCEDURES

2.1. Step 1: The Modified End-Coupled Structure

Figure 1(a) showed the basic end-coupled microstrip line structure, where the upper microstrip line was a λ/2 cross coupling resonator with operating frequency of 5.5 GHz, and the simulated result of return loss was shown in Figure 2(a). For the purpose of the insertion of transmission zeros between the pass bands, the modified end-coupled microstrip line structure with a λ/2 cross coupling resonator was introduced, as Figure 1(b) showed. Although the total length of the upper λ/2 cross coupling resonator was unchanged, as D of the resonator fixed at 0.4 mm and the L increased gradually, because of the variation of coupling, it was found that two transmission zeros were generated as L was greater than 3 mm, and the ripple of the first harmonic could be reduced effectively, which revealed a phenomenon of $f_1/f_0 > 2$. Figure 2(b) showed a better modified end-coupled wideband filter with a λ/2 cross coupling resonator ($L = 2$ mm and $D = 2.4$ mm), the stop-band rejection between two pass bands was −44 dB, and the depth of transmission zeros were −83 and −60 dB, respectively. However, the major drawback for this structure was that the upper skirt of 5.2 GHz was still not good enough.

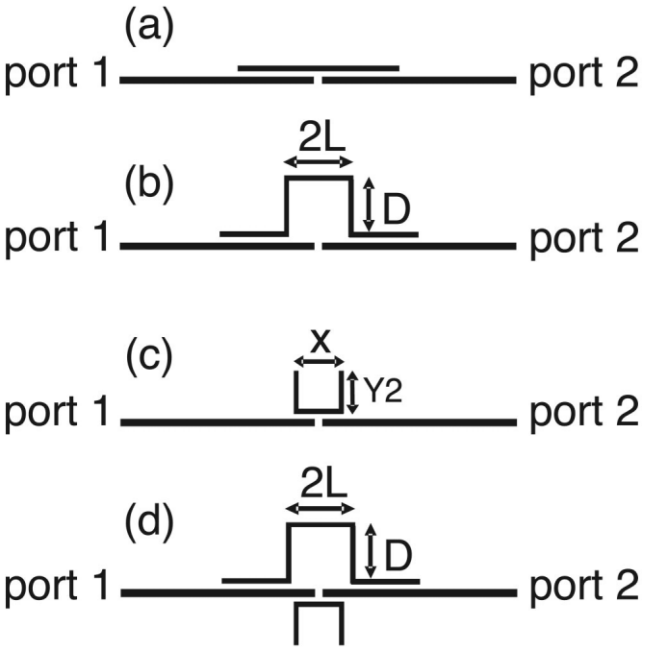

Figure 1 The structures of the designed wideband filter

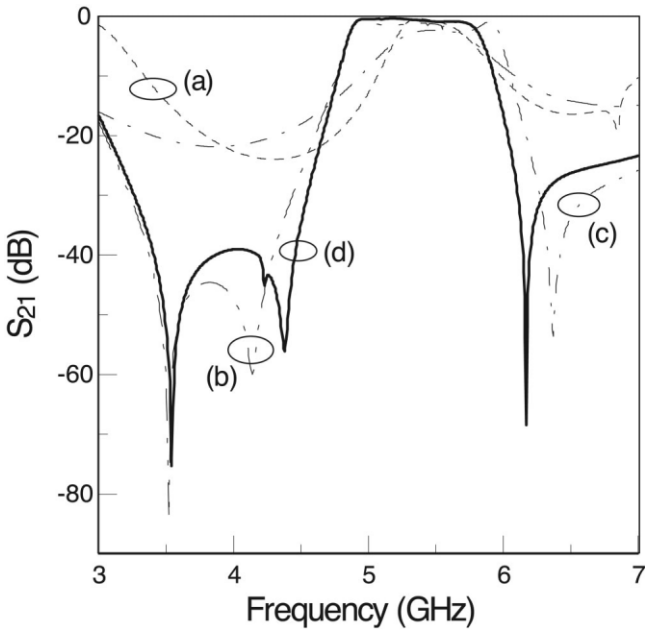

Figure 2 Simulated S_{21} results of the different designed structures

2.2. Step 2: Using a λ/2 Hairpin Resonator to Generate a Zero

Figure 1(c) shows end-coupled microstrip line structure with a λ/2 hairpin resonator (resonated frequency 5.2 GHz), owing to the variation of coupling and the variation of the λ/2 hairpin resonator, a transmission zero generated at the upper skirt of 5.2 GHz as the size of resonator (X and $Y2$) increased, which could be used to low down the upper skirt of 5.2 GHz in Figure 2(b). As $Y2$ fixed at 1.8 mm and X increased, the zero would move toward lower frequency, furthermore, the depth of zero increased as X increased, the variation of coupling would be the reason. As X was fixed at 2.6 mm and $Y2$ increased, the zero would move toward lower frequency, too. For $X = 2.6$ mm and $Y2 = 1.8$ mm the designed filter would have the optimal characteristics.

2.3. Step 3: Combining Above Two Structures

To improve the upper skirt in Figure 2(c), a λ/2 U-shaped hairpin resonator was added into the modified end-coupled microstrip line structure to conquer the disadvantage. The λ/2 hairpin resonator was added on the other side of the couple line, as shown in Figure 1(d), as the length of $Y2$ increased gradually, a transmission zero would be generated at the right-side of 5.2 GHz, and that would improve the upper skirt of 5.2 GHz obviously.

3. THE FABRICATION OF THE FILTERS ON THE $MGTA_{1.5}NB_{0.5}O_6$ CERAMIC SUBSTRATE

The parameters of the proposed filter were showed in Figure 3, the size of this filters was only 26.3 mm ×5.5 mm. The mask was designed according to the simulated patterns, and then the Ag/Pd paste was used to print the filter patterns on the $MgTa_{1.5}Nb_{0.5}O_6$ ceramic substrates by a screen printer. Then the printed pattern was fired under the condition 800°C/30min in an oven. Finally, two SMA connectors were soldered to each filter, and the characteristics of the filters were measured by an impedance analyzer (HP-8720). The simulated and measured results of the fabricated filter are compared in Figure 4. For simulation, the bandwidth was 18.6% (970 MHz), and insertion loss is 0.38 dB; and for measurement, the bandwidth was 18.3% (955 MHz), and insertion loss is

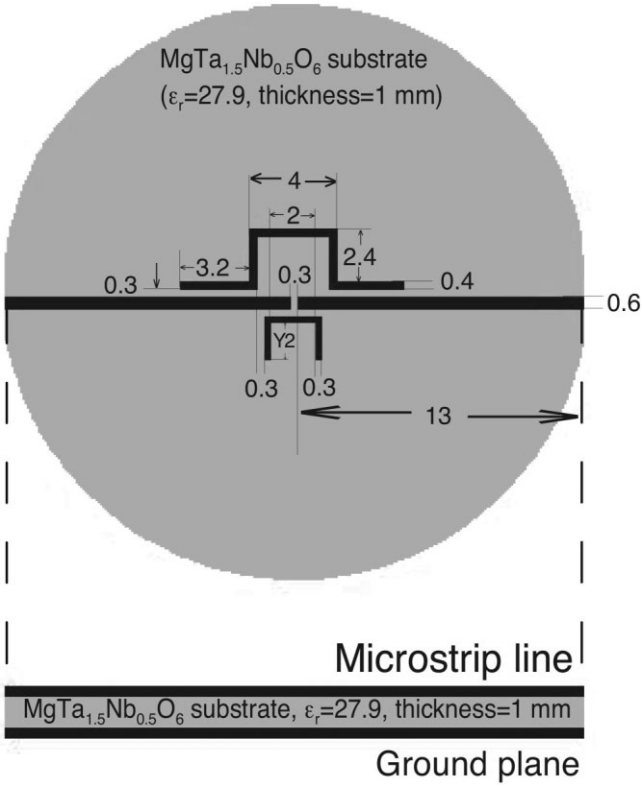

Figure 3 The parameters of the proposed filter

0.72 dB, which is suitable for the use of modern communication systems.

4. CONCLUSIONS

In this article, three deeply transmission zeros (−75 dB, −56 dB, −68 dB) are inserted to modify the characteristic of the filters, whereas two zeros are located in the stopbands, and the third zero is located at the upper skirt of 5.2 GHz, all these zeros improve the characteristics of stop-band obviously. The insertion loss of the filters was all smaller than 0.8 dB because of the use of high quality factor ceramic substrates and the combination coupling method. The basic end-coupled microstrip line structure was combined to a λ/2 cross coupling resonator and a λ/2 hairpin resonator, a miniature wideband filters had been accomplished on the $MgTa_{1.5}Nb_{0.5}O_6$ microwave dielectric ceramic substrate.

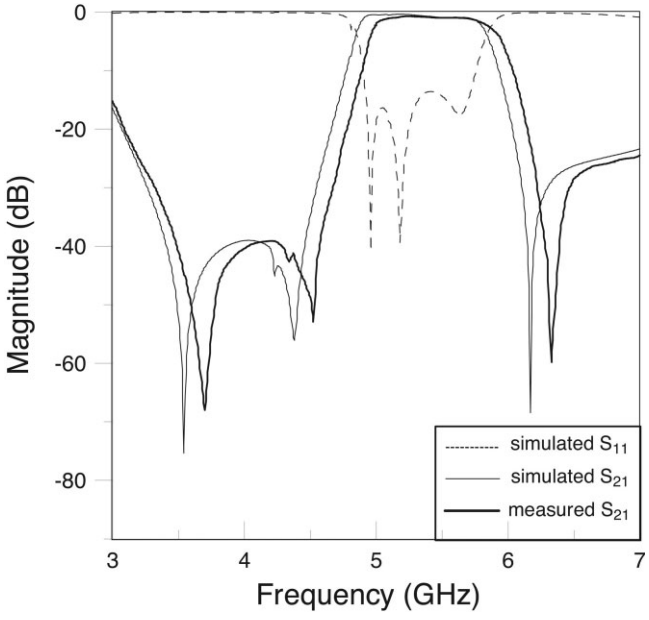

Figure 4 Simulated and measured results of the filters

REFERENCES

1. J.T. Kuo, C.L. Hsu, and E. Shih, Compact planar quasi-elliptic function filter with inline stepped-impedance resonators, IEEE Trans Microwave Theory Tech 55 (2007), 1747–1755.
2. C.M. Tsai and H.M. Lee, Improved design equations of the tapped-line structure for coupled-line filters, IEEE Microwave Wireless Compon Lett 17 (2007), 244–246.
3. S. Sun and L. Zhu, Coupling dispersion of parallel-coupled microstrip lines for dual-band filters with controllable fractional pass bandwidths, In: 2005 IEEE MTT-S International Microwave Symposium Digest, Long Beach, CA, June 2005, pp. 2195–2198.
4. C.K. Liao and C.Y. Chang, Modified parallel-coupled filter with two independently controllable upper stopband transmission zeros, IEEE Microwave Wireless Compon Lett 15 (2005), 841–843.
5. R.M. Kurzrok, General four-resonator filters at microwave frequencies, IEEE Trans Microwave Theory Tech MTT-14 (1996), 295–296.
6. C.M. Cheng, Y.C. Chen, C.F. Yang, and C.C. Chan, Sintering and compositional effects on the microwave dielectric characteristics of $Mg(Ta_{1-x}Nb_x)_2O_6$ ceramics with $0.25 \leqq x \leqq 0.35$, J Electroceram 18 (2007), 155–160.

A NOVEL 2.4 GHz AND 6.8 GHz DUAL-BAND TRANSMITTER USING DEFECTED GROUND STRUCTURE

Xiaoqun Chen, Xiaowei Shi, Yuchun Guo, and Changmin Xiao
National Laboratory of Antennas and Microwave Technology, Xidian University, Xi'an 710071, Shaanxi, China; Corresponding author: xqchen@mail.xidian.edu.cn

Received 13 April 2008

ABSTRACT: *A novel dual-band module transmitter is presented in this article. It works as a power amplifier at 2.4 GHz that satisfies the 802.11b/g wireless LAN standard and performs as an active frequency doubler at 6.8 GHz with the stop band characteristics of defected ground structure (DGS). The equivalent circuit unit and the stop band characteristics of the microstrip DGS are analyzed and simulated. For the proposed transmitter, second harmonic suppression is below −52.6 dBc in the amplifier mode, and fundamental suppression is below −41 dBc in the frequency doubler mode. It achieves 13.7 dBm of P1 dB and its gain is 16.5 dB at amplifier mode, and its maximum output is 7.8 dBm at 6.8 GHz in frequency double mode.* © 2008 Wiley Periodicals, Inc. Microwave Opt Technol Lett 50: 3225–3228, 2008; Published online in Wiley InterScience (www.interscience.wiley.com). DOI 10.1002/mop.23935

Key words: *dual band transmitter; frequency doubler; power amplifier; DGS*

1. INTRODUCTION

High speed wireless LAN technology is crucial in modern communication system, and it propagates rapidly in the infrastructure of office and home environments. In 2002, the IEEE extended the 802.11b standard to higher data rates up to 54 Mbps in the 2.4 GHz